Hindawi
Geofluids
Volume 2023, Article ID 9706407, 12 pages
https://doi.org/10.1155/2023/9706407

Research Article

Transient Coupled Flow Model for Matrix-Fracture in High-Pressure Gas Reservoirs Opened by Gas Drilling

Jiajie Liu ,[1] Gao Li,[2] Zhi Ye,[3] Wang He,[4] and Zhihao Zeng[5]

[1]*College of Chemistry and Chemical Engineering, Shaanxi Key Laboratory of Chemical Additives for Industry, Shaanxi University of Science & Technology, Xi'an 710021, China*
[2]*State Key Laboratory of Oil and Gas Reservoir Geology and Exploration, School of Petroleum Engineering, Southwest Petroleum University, Chengdu 610500, China*
[3]*Xi'an Changqing Chemical Group Co., Ltd. of CNPC Changqing Oilfield Branch, Xi'an 710299, China*
[4]*Engineering Technology Management Department of CNPC Changqing Oilfield Branch, Xi'an 710018, China*
[5]*Engineering Technology Research Institute of PetroChina Southwest Oil & Gasfield Company, Chengdu 610017, China*

Correspondence should be addressed to Jiajie Liu; liujiajie@sust.edu.cn

Received 26 May 2022; Revised 11 November 2022; Accepted 24 November 2022; Published 10 February 2023

Academic Editor: Dengke Liu

Gas drilling technology is an effective method to protect low permeability tight sandstone reservoirs from damage. However, using this technology to drill high-pressure fractured reservoirs, the fluid flow characteristics are extremely complex, leading to drilling safety challenges. Therefore, based on the conservation equations of mass, momentum, and energy, a new transient coupled flow model in matrix-fracture is established for high-pressure gas reservoirs opened by gas drilling, considering convection term and energy equation, to research the pressure and flow velocity transient behaviors. This model is solved by Shaher Momani's algorithm and CyabJiBe format, and the type curves of the pressure and flow velocity are plotted. The three flow stages are developed, and the impact of parameters and equation terms on the transient flow behavior is analyzed and discussed, such as the energy equation, the matrix permeability (k), the fracture aperture (L_f), and the fracture outlet pressure. It is found that the energy equation term of the model has a great influence on the transient characteristics such as velocity and pressure, which cannot be ignored. In the first flow stage, the flow velocity characteristics are not affected by the matrix parameters being extremely unstable, but in the second and third stages, the influence of the gas supplied to fracture cannot be ignored. The proposed transient coupled flow model provides a new understanding of the transient flow behavior in matrix-fracture for high-pressure reservoirs during gas drilling, which can be used to interpret the characteristics of pressure and velocity more realistically, to provide support for safe drilling of gas drilling.

1. Introduction

The development of high-pressure tight gas reservoirs is an unsolved problem in the petroleum industry due to the low productivity and high pressure of gas wells. Producing gas from tight reservoirs presents a unique challenge due to the contamination of water from the fracturing and drilling fluids [1–3]. As an advanced drilling technology, using air as a drilling fluid began in the 1950s [4–6]. Gas drilling technology has shown to be promising to solve the problem, which is characterized by the easier discovery of reservoirs, low reservoir damage, and increased rate of penetration [7, 8]. However, there are many problems during practice, especially the safety of gas drilling, which is very uncontrollable in many areas due to the lack of understanding of the transient flow law and pressure characteristics of high-pressure gas, when the high-pressure reservoir is opened by gas drilling [9, 10]. Therefore, it is very important for gas drilling engineers to understand the flow characteristics of gas in fractured high-pressure reservoirs.

A matrix-fracture medium model is commonly used for natural fracture gas reservoirs. Warren and Root have developed a dual-porosity medium model, which is based on the assumption that the matrix is the main storage space, the natural fractures are the main seepage channels, and the matrix provides a gas source to fracture [11–13]. Kazemi et al. have developed a double-porosity dual-permeability model; the gas of the matrix system and small-scale fractures not only can provide a gas source to fracture but also can provide a gas source to the wellbore [14]. Although there are abundant studies of the coupled flow behavior for matrix-fracture reservoirs, few models research the characteristics of unstable complex flow for high-pressure reservoirs during gas drilling.

For naturally fractured gas reservoirs, most researchers have focused on transient flow behaviors. Slimani and Tiab [15] established a theoretical model, to investigate the influence of transient flow behaviors on type curves for partially penetrating vertical wells in naturally fractured reservoirs. Wu et al. researched a triple-porosity medium model to analyze the fluid flow behavior in matrix-fracture-cave reservoirs [16]. Du et al. conducted a multiregion composite model, to investigate the transient flow behavior for fractured-cave reservoirs [17]. For composite fractured gas reservoirs, Nie et al. [18] studied a transient flow model with the high-velocity non-Darcy effect, to simulate the non-Darcy flow for the inner region as a dual-porosity medium, and the Darcy flow for the outer region as a homogeneous medium.

With the development of hydraulic fracturing technology, which is one of the effective ways to develop tight sandstone and shale reservoirs with low permeability characteristics, many researchers attach importance to the study of complex fluid behaviors in such reservoirs [19]. For a hydraulic fractured sandstone tight reservoir, a series of new fluid flow models are presented to help engineers understand the transient pressure characteristics of gas flow. A new mathematical model has been proposed to study the transient pressure characteristics for hydraulic fractured wells with nonuniform fracture geometry and permeability [20]. The semianalytical model has been established and solved to analyze the transient pressure behavior for a fractured vertical well with hydraulic/natural fracture networks by considering stress-sensitive effects [21]. The model for multistage fractured horizontal wells with discretely distributed natural fractures has been researched to investigate pressure performance [22]. The new fractally fractional diffusion model of composite dual-porosity has been developed to evaluate the performance of multiple fractured horizontal wells with stimulated reservoir volume in tight gas reservoirs [23]. The discrete fracture-matrix method based on the numerical well testing model has been proposed to study the pressure transient responses of discretely distributed natural fractures [24]. Due to the characteristics of ultralow porosity and ultralow permeability in shale gas fields, which contain both adsorbed gas and free gas, hydraulic fracturing technology and horizontal well technology are commonly used in shale gas development. In recent years, discrete fracture models have been vigorously developed to study gas seepage in gas reservoirs in shale [25, 26], and many scholars believe that the changes in matrix permeability and fracture permeability with increasing effective stress cannot be ignored [27, 28]. A series of multiple-porosity model transient flow models are proposed, including the dual-porosity dual-permeability model and triple-porosity model, to study the transient pressure behaviors [29, 30]. Although there are abundant studies of transient flow behavior for naturally and hydraulically fractured reservoirs, few models mentioned above have touched on the convection term and considered the influence of the energy equation.

In fact, owing to the high pressure of the reservoirs and high conductivity of the fractures, the transient flow of gas cannot ignore the influence of the gas convection term and energy equation. Based on the law of conservation of mass, momentum, and energy, a transient coupled flow in matrix-fracture for the high-pressure reservoirs opened by gas drilling model is established. The flow in fracture is considered as a radial flow to simulate the convection and diffusion process of gas, and the flow in matrix reservoir is considered a parallel seepage into fracture to simulate the non-Darcy flow, as shown in Figure 1. By using Shaher Momani's algorithm and CyabJiBe format, the analytical solution of the coupled transient flow in matrix-fracture model can be obtained [31–33]. Then, the type curves with the influence of energy conversion and physical characteristics of matrix-fracture are plotted.

2. Physical Model and Assumptions

Figure 1 is the schematic of the physical model, which represents the gas transient flow process in fractured reservoirs opened by gas drilling with no damage. The gas flow in reservoirs is divided into two regions, which have different flow characteristics and different reservoir characteristics. The first gas flow area is the gas transient radial flow at high velocity from fracture to wellbore, considering the convective and diffusion terms. The second gas flow area is the gas transient parallel flow perpendicular to the fracture from the matrix. The main assumptions of this model are the following: (1) The fracture has the same geometric characteristics. (2) In the second flow area, the matrix with homogeneous characteristics provides a gas source to fracture vertically. (3) The permeability of the matrix is independent of pressure. (4) The influence of the secondary gradient on the flow in the matrix is ignored.

3. Mathematical Model

3.1. Mathematical Model for the Gas Transient Parallel Flow Perpendicular to Fracture from Matrix. Owing to the high pressure of the reservoirs, the influence of non-Darcy flow cannot be ignored for the gas flow in the matrix; the equation is as follows [18]:

$$-\frac{dp}{dz_m} = \frac{K}{\mu} v + \beta \rho v^n. \tag{1}$$

In Equation (1), K represents the selected reservoir matrix permeability. v and μ represent gas velocity and viscosity. ρ represents gas density. n represents the value related to the properties of the porous medium. β represents the non-Darcy flow factor.

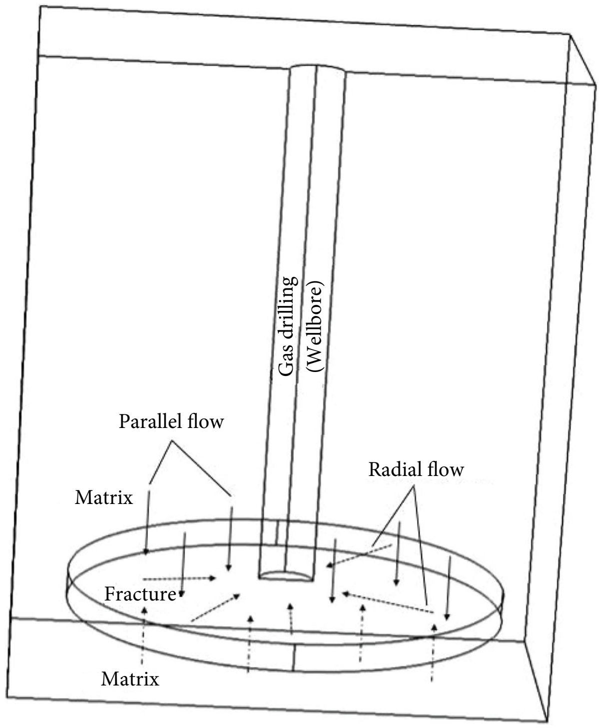

Figure 1: Physical model of gas flow process in matrix-fracture reservoirs opened by gas drilling.

For plane flow in homogeneous formation, Equation (1) can be rewritten as follows:

$$v = -\delta \frac{K}{\mu} \frac{\partial p}{\partial z_m}. \quad (2)$$

In Equation (2), δ represents the inertial-turbulence correction coefficient factor and z_m represents vertical distance.

The continuity equation of gas transient parallel flow perpendicular to fracture from the matrix is as follows:

$$\frac{\partial(\rho\phi)}{\partial t} + \frac{\partial(\rho v)}{\partial z_m} = 0. \quad (3)$$

Binding Equation (2), Equation (3) can be written as follows (the detailed derivation of Equation (4) is presented in the appendix:

$$\frac{\partial p^2}{\partial {z_m}^2} = \frac{\phi\mu C_g}{\delta K} \frac{\partial p}{\partial t}. \quad (4)$$

3.2. Mathematical Model for the Gas Transient Radial Flow from Fracture to Wellbore. In the study of transient radial flow in fracture, the influence of the convection term and energy equation is mostly ignored; the transient flow characteristics cannot be truly reflected. Therefore, the convection term and energy equation are introduced to describe the transient flow characteristics of natural gas in fractures, during the instantaneous opening of fractured reservoirs by gas drilling. The transient mathematical model of gas transient radial flow in fractures is established.

The governing equations of the model are as follows (the detailed derivation of Equations (5)–(7) is presented in the appendix) [34–36].

The continuity equation is as follows:

$$\frac{\partial \rho}{\partial t} + \frac{\partial r\rho v_r}{r\partial r} = 0. \quad (5)$$

The momentum conservation equation is as follows:

$$\frac{\partial \rho v_r}{\partial t} + \frac{\partial r(\rho v_r v_r + p - \tau_{rr})}{r\partial r} = \frac{p}{r}. \quad (6)$$

The energy conservation equation is as follows:

$$\frac{\partial \rho E}{\partial t} + \frac{\partial r(\rho H v_r - v_r\tau_{rr} + q_r)}{r\partial r} = \rho q. \quad (7)$$

In the equation, energy $E = CvT + 1/2{v_r}^2$, enthalpy $H = CpT + 1/2{v_r}^2 = E + p/\rho$, radial flow $q_r = -\lambda_g \partial T/\partial r$, and tangential stress $\tau_{rr} = 2/3\mu(2\partial r v_r/r\partial r) - 2\mu v_r/r$.

3.3. Mathematical Model for Transient Coupled Flow Model in Matrix-Fracture. The transient coupled flow model in matrix-fracture is applied to describe and analyze the coupling flow characteristics of gas in matrix and fracture, when the fractured reservoir is opened by gas drilling, including the radial flow characteristics of gas from fracture to wellbore and the flow characteristics of gas flowing vertically from matrix to fracture. The gas source is continuously supplied from matrix to fracture with the decrease of fracture pressure. And the convection term and energy equation are introduced to the transient coupled flow model. The physical model is shown in Figure 1.

According to Equations (5)–(7), governing equations of the model are shown in Equations (8)–(10).

Continuity equation for transient coupled flow in the matrix-fracture system [34–36]:

$$\frac{\partial \rho}{\partial t} + \frac{\partial r\rho v_r}{r\partial r} = \dot{q}. \quad (8)$$

In Equation (8), $\dot{q}$ represents the gas source which is continuously provided from matrix to fracture.

Momentum conservation equation for transient coupled flow in the matrix-fracture system:

$$\frac{\partial \rho v_r}{\partial t} + \frac{\partial r(\rho v_r v_r + p - \tau_{rr})}{r\partial r} = \frac{p}{r}. \quad (9)$$

The energy conservation equation for transient coupled flow in the matrix-fracture system:

$$\frac{\partial \rho E}{\partial t} + \frac{\partial r(\rho H v_r - v_r\tau_{rr} + q_r)}{r\partial r} = \rho q. \quad (10)$$

3.4. Mathematical Model Solutions. In this section, Equations (7)–(9) are rewritten as the vector form of the convection diffusion equation; the mathematical model is as follows:

$$\frac{\partial u}{\partial t} = -a\frac{\partial u}{\partial r} + b\frac{\partial^2 u}{\partial r^2} + f(r,t). \tag{11}$$

The vector parameter $u, a, b, c, f(r,t)$ in Equation (11) are as follows:

$$u = \begin{vmatrix} p \\ v_r \\ T \end{vmatrix},$$
$$a = \begin{vmatrix} v_r & \rho & 0 \\ 1 & \left(pv_r - \frac{2}{3}\frac{\mu}{r\rho}\right) & 0 \\ 0 & \left(p + \frac{2}{3}\frac{\mu v_r}{r}\right) & pv_r Cv \end{vmatrix},$$
$$b = \begin{vmatrix} 0 & 0 & 0 \\ 0 & \frac{4}{3}\frac{\mu}{\rho} & 0 \\ 0 & 0 & 0 \end{vmatrix},$$
$$f(x,t) = \begin{vmatrix} \frac{\dot{q}p}{\rho} - \frac{pv_r}{r} \\ 0 \\ pq - \frac{pv_r}{\rho r} \end{vmatrix}. \tag{12}$$

Shaher Momani's algorithm and CyabJiBe format for solving the convection-diffusion equation with a nonlinear source term is used to address the mathematical model. The basic definitions of the algorithm are as follows.

Definition 1.

$$Jf(r) = \frac{1}{\Gamma}\left(\int_o^z f(t)\right)dt. \tag{13}$$

In the equation, J can be found in [37].

Definition 2.

$$Df(x) = J^m D^m f(x) = \frac{1}{\Gamma(m)}\int_0^x (x-t)^{m-2} f^{(m)}(t)dt. \tag{14}$$

Differential operator D is described in detail in Reference [38].

Definition 3.

$$L_x = \frac{\partial}{\partial x},$$
$$L_{xx} = \frac{\partial^2}{\partial x^2},$$
$$D_t = \frac{\partial}{\partial t}. \tag{15}$$

Shaher Momani's algorithm for solving the convection-diffusion equation consists in finding the solution in the form:

$$u(r,t) = \sum_{n=0}^{\infty} u_n(r,t). \tag{16}$$

The operator J and the inverse of the operator D are applied to solve Equation (11):

$$u(r,t) = \sum_{k=0}^{m-1}\frac{\partial^k u}{\partial t^k}(r,0^+)\frac{t^k}{k!} + Jf(r,t) + bJL_{rr}u(r,t) - aJL_r u(r,t). \tag{17}$$

The components u_n recursively is defined as follows:

$$u_0(r,t) = \sum_{k=0}^{m-1}\frac{\partial^k u}{\partial t^k}(r,0^+)\frac{t^k}{k!} + Jf(r,t), \tag{18}$$

$$u_1(r,t) = bJL_{rr}u_0 - aJL_r u_0, \tag{19}$$

$$u_{n+1}(r,t) = bJL_{rr}u_n - aJL_r u_n. \tag{20}$$

The exact series solution Equation (16) is defined by Equations (18)–(20), which give an approximate solution to Equation (11). Finally, the standard characteristic curves of fluid velocity with time and pressure with space in fracture can be plotted by Mathcad as computing software, when the fractured reservoir is opened by gas drilling.

4. Results and Discussion

4.1. Flow Stage Analysis. The conditions of the model are as follows.

The outer boundary pressure of the matrix reservoir is constant pressure $p_i = 60$ MPa. The inner boundary pressure of the matrix $p_m l_{z=0} = p$ is the dynamic boundary pressure, which is the outer boundary pressure of the fracture. The inner boundary pressure of the fracture is the constant pressure $p_m l_{r=0} = 58$ MPa. The matrix permeability is 0.01 mD.

Figure 2 shows the velocity behavior characteristics of coupled flow for matrix-fracture in a high-pressure reservoir for gas drilling. The three flow stages can be represented by curves. Figure 3 shows the amplification characteristic curve of the first flow stage.

The first stage describes gas velocity characteristic in the fractured reservoir, which is opened by gas drilling instantaneously. The magnification curve is shown in Figure 3. In

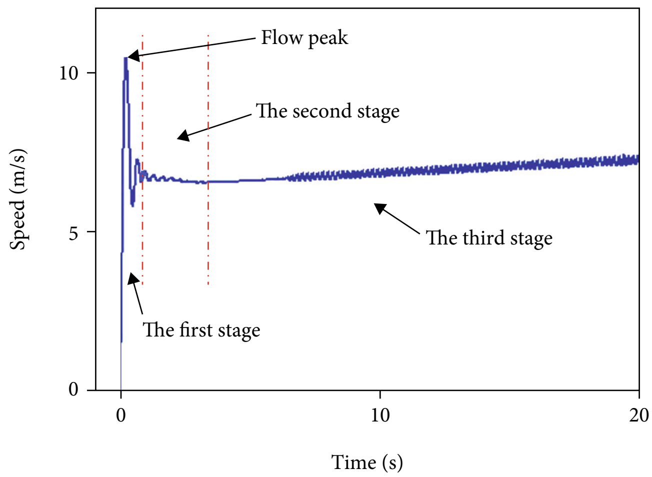

Figure 2: Three-stage characteristics of transient coupled flow in matrix-fracture.

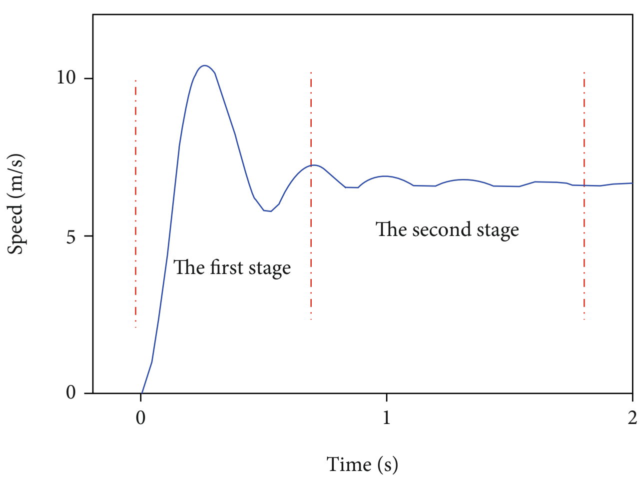

Figure 3: Magnification curve of the first and second stage characteristics of transient coupled flow in matrix-fracture.

this flow stage, the gas flow velocity in fracture is much higher than that of the second and third stages, it is extremely unstable, and it may have a huge impact on the safety of the bottom hole. The flowing gas mainly comes from the gas stored in fracture, and the matrix will not provide gas to the fracture. Because the total amount of gas stored in the fracture of reservoirs is much less than that in the matrix, the duration of the flow process is extremely short, which is less than 1 second.

In the second stage, the flowing gas in the fracture mainly includes the gas from the reservoir in the fracture and the gas supplied by the matrix to the fracture. The gas flowing velocity drops rapidly, and it is quasisteady flow. The third stage reflects the flow characteristics of the stable flow stage. The flowing gas in the fracture is supplied mainly from the matrix. In this process, the pressure and the flow velocity drop very slowly.

Figure 4 shows the characteristics of the pressure funnel in fracture from 0.05 seconds to 1 second after being opened by gas drilling. The pressure attenuation mainly exists in the fracture near the wellbore, that is, within 10 m from the wellbore. The closer to the wellbore, the more serious the pressure attenuation. As time goes on, the pressure in the fracture becomes lower and lower. The pressure drop is mainly consumed near the wellbore, during the fluid flowing from the reservoir edge to the bottom of the well.

4.2. Impact of the Parameters. In this section, the characteristic parameters of the transient coupled flow model in the matrix-fracture reservoir are analyzed in detail, including the influence of the energy conversion, the matrix permeability k, the fracture aperture L_f, and the fracture outlet pressure p. These parameters have different influences on the characteristics of gas flow velocity and pressure in the fracture, as shown in Figures 5–9.

4.2.1. Influence of the Energy Conversion. Figure 5 compares the influence of considering energy equation and without energy equation on curves of the transient coupled flow in matrix-fracture model. As a compressible fluid, the gas flow process has the conversion of kinetic energy and internal energy under the condition of high pressure difference and high flow velocity, as shown in Figure 5, by comparing the flow velocity in fracture without considering the energy conversion and considering the energy conversion. In the first stage, it is found that if the energy conversion process is ignored, the flow velocity cannot peak rapidly when the fracture is opened by gas drilling but rises slowly, and the characteristics of the curve cannot reflect the real flow situation. In the second and third flow stages, the characteristics of flow velocity without considering energy conversion are higher than those considering energy conversion. In the condition of high velocity of gas flow in the fracture, the part of kinetic energy can be converted into internal energy. According to the law of energy conservation, the velocity of gas flow decreases due to the reduction of kinetic energy. Therefore, the effect of energy conversion cannot be ignored in the study of the characteristics of gas flow at high velocity for high-pressure reservoirs.

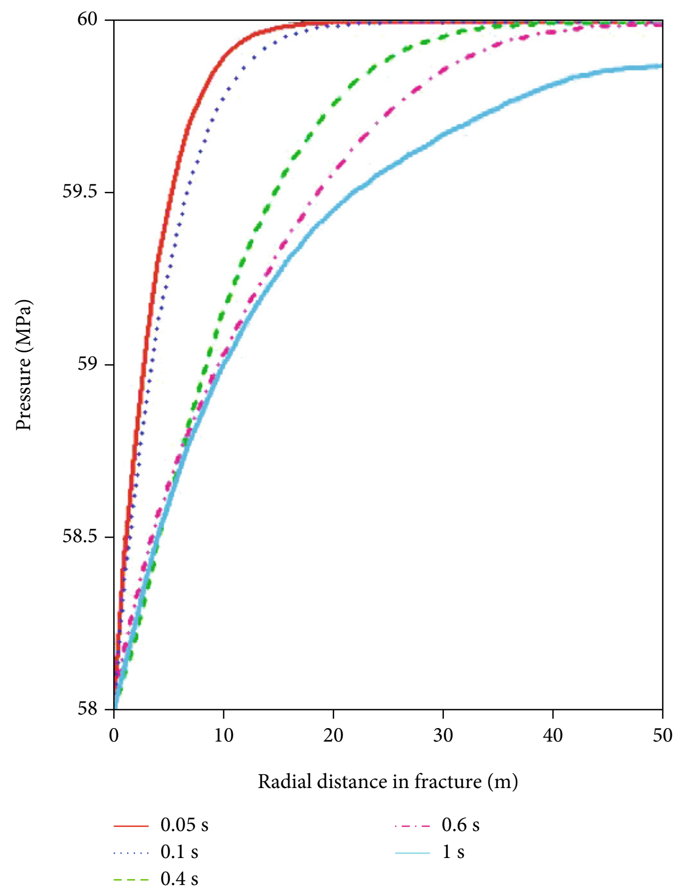

FIGURE 4: Radial pressure drop funnel in fracture.

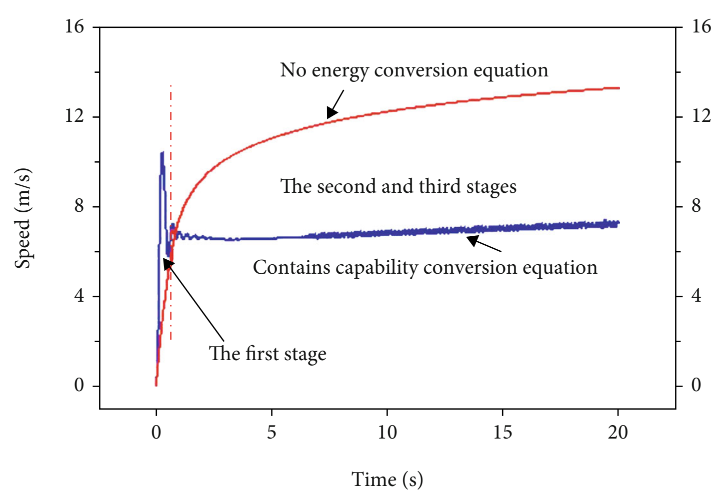

FIGURE 5: Influence of energy conversion equation.

4.2.2. Impact of the Matrix Permeability (k). Figure 6 shows the influence of different matrix permeability (k) on the curves of flow velocity with time in fracture simulated by the transient coupled flow model. The values of the matrix permeability (k) are shown in Figure 6. Due to the fracture supplied with a source of gas from the matrix, it can be observed that the matrix permeability mainly influences the second and third flow stages of the type curves for the transient coupled flow model. In these two flow stages, when the matrix permeability (k) is increased, the flow velocity curves rises. On the contrary, if the matrix permeability (k) is decreased, the flow velocity curves goes down. In the first flow stage, the matrix permeability cannot affect the flow characteristic of the transient coupled flow model; the main

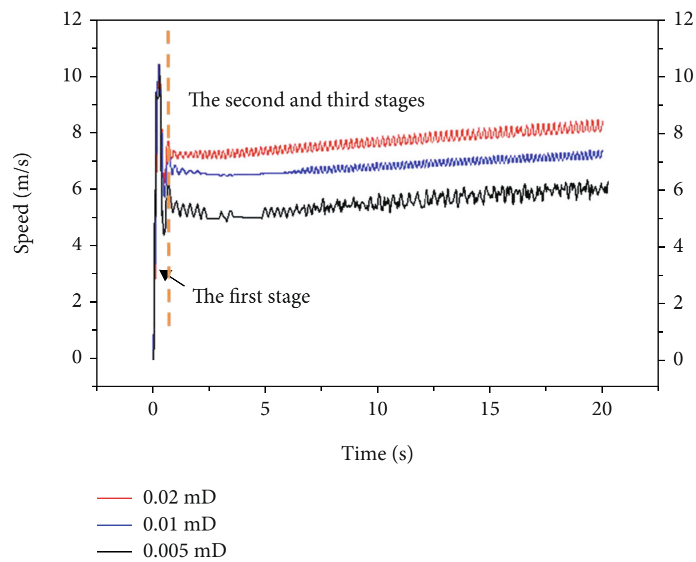

Figure 6: Influence of matrix permeability (k).

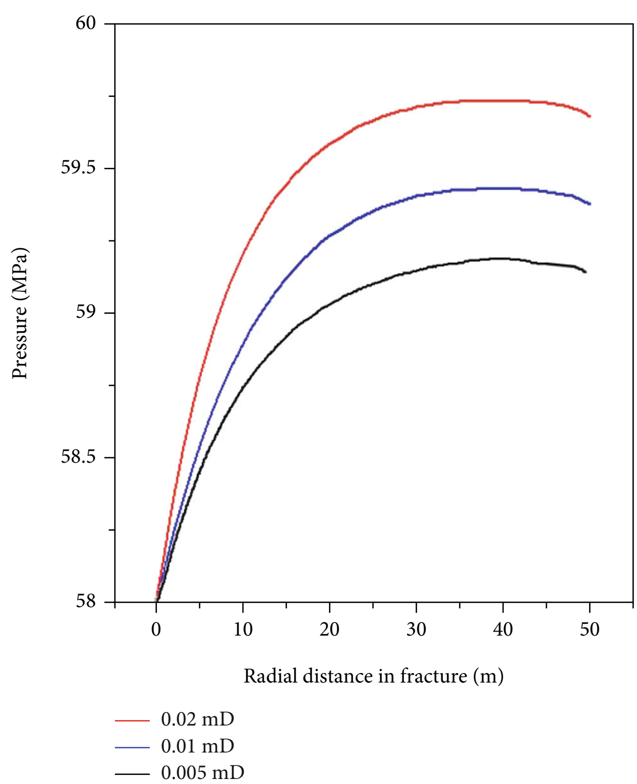

Figure 7: Influence of matrix permeability (k) on pressure drop funnel in fractures.

reason is that the flowing gas mainly comes from the gas source stored in the fracture, while the gas in the matrix does not flow.

Figure 7 illustrates the impact of matrix permeability (k) on the curves of the pressure drop funnel in fracture for the transient coupled flow model. The values of matrix permeability (k) are shown in Figure 7. The characteristic curves of the pressure drop funnel also shows that matrix permeability (k) affects the attenuation of fracture pressure. The larger the matrix permeability (k), the slower the fracture pressure falls. If the matrix permeability (k) is increased, the supply of gas from the matrix to the fracture can increase, so the rate of pressure drop decreases.

4.2.3. Impact of the Fracture Aperture L_f. Figure 8 shows the influence of different fracture aperture (L_f) on the curves of flow velocity with time in fracture simulated by the transient coupled flow model. The values of the fracture aperture (L_f) are shown in Figure 8. The curves also illustrate that the fracture aperture (L_f) influences the overall three flow stages. The larger the fracture aperture (L_f), the higher the instantaneous peak for gas production in the first stage and the greater the gas velocity in the second and third fracture flow stages. Therefore, the larger the fracture aperture (L_f) encountered during gas drilling, the greater the impact on the wellbore safety. The reason is that the smaller the fracture aperture, the smaller the flow channel and the greater the flow resistance.

4.2.4. Influence of the Fracture Outlet Pressure. Figure 9 illustrates the influence of the fracture outlet pressure on the curves of flow velocity with time in fracture for the transient coupled flow model. The parameters of the fracture outlet pressure are shown in Figure 9. It can be seen in the curves of flow velocity with time; the fracture outlet pressure influences the overall three flow stages during gas drilling. Undoubtedly, the fracture outlet pressure determines the driving force of the flow system, including gas flow system from matrix to fracture and gas flow system from fracture to wellbore. The lower the fracture outlet pressure, the higher the driving force of the fluid system, the more gas supplied from matrix to fracture, and the greater the gas flow velocity in the fracture.

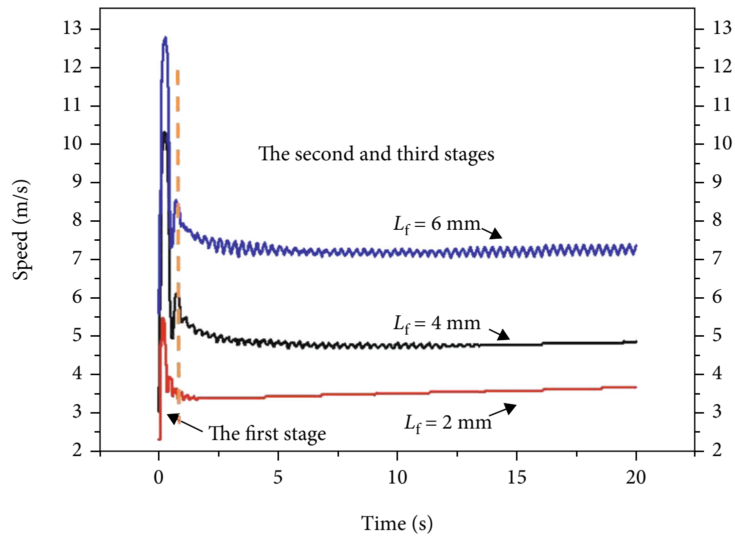

FIGURE 8: Influence of fracture aperture L_f.

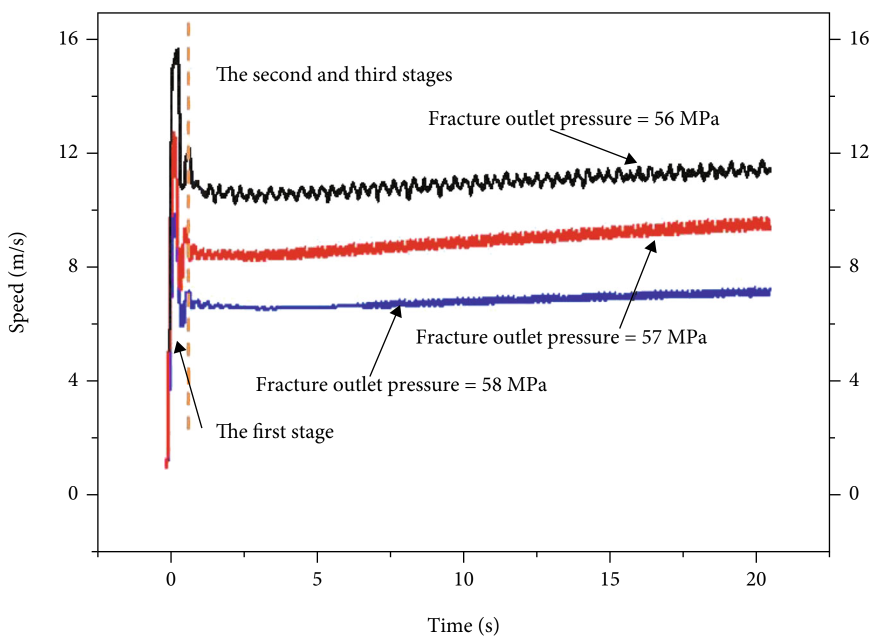

FIGURE 9: Influence of fracture outlet pressure.

5. Conclusions

(1) A new transient coupled flow model is established for matrix-fracture in high-pressure reservoir during gas drilling, based on the laws of conservation of mass, momentum, and energy

(2) The model considers more realistic assumptions about the convection term and the energy equation and reflects the more real transient flow characteristics

(3) The model is solved by using Shaher Momani's algorithm and CyabJiBe format. The standard pressure and velocity characteristic curves of the proposed flow model are drawn into three flow regimes. In the first stage, the characteristics of pressure and flow velocity in fracture are extremely unstable, with a rapid emergence of peak, and the gas flowing from the fracture to the wellbore mainly comes from the gas stored in the fracture, without matrix gas. In the second and third flow stages, the flow characteristics are relatively stable

(4) The characteristic parameters of the transient coupled flow model are also analyzed for high-pressure fractured reservoirs opened by drilling. It is found that the pressure and velocity characteristics are mainly affected by the matrix permeability (k),

the fracture aperture (L_f), and the fracture outlet pressure. Different characteristic parameters have different influences on the type curves

Appendix

Governing Equation

In this section, a detailed derivation of the governing equation of the gas transient radial flow from fracture to the wellbore region is provided.

(1) The three-dimensional N-S equation of compressible fluid is as follows [34–36]:

$$\frac{\partial U}{\partial t}+\frac{\partial (E-V_x)}{\partial x}+\frac{\partial (F-V_y)}{\partial y}+\frac{\partial (G-V_z)}{\partial z}=0. \quad \text{(A.1)}$$

The vector parameter $U, E, F, G, V_x, V_y, V_z, \tau_{xx}, \tau_{yy}, \tau_{zz}, \tau_{xy}, \tau_{xz}, q_x, q_y, q_z$ in Equation (A.1) are as follows:

$$U=\begin{pmatrix}\rho\\ \rho u_x\\ \rho u_y\\ \rho u_z\\ \rho E\end{pmatrix},$$

$$E=\begin{pmatrix}\rho u_x\\ \rho u_x u_x+p\\ \rho u_y u_x\\ \rho u_z u_x\\ \rho H u_x\end{pmatrix},$$

$$F=\begin{pmatrix}\rho u_y\\ \rho u_x u_y\\ \rho u_y u_y+p\\ \rho u_z u_y\\ \rho H u_y\end{pmatrix},$$

$$G=\begin{pmatrix}\rho u_z\\ \rho u_x u_z\\ \rho u_y u_z\\ \rho u_z u_z+p\\ \rho H u_z\end{pmatrix},$$

$$V_x=\begin{pmatrix}0\\ \tau_{xx}\\ \tau_{yx}\\ \tau_{zx}\\ u\tau_{xx}+v\tau_{yx}+w\tau_{zx}-q_x\end{pmatrix},$$

$$V_y=\begin{pmatrix}0\\ \tau_{xy}\\ \tau_{yy}\\ \tau_{zy}\\ u_x\tau_{xy}+u_y\tau_{yy}+u_z\tau_{zy}-q_y\end{pmatrix},$$

$$V_z=\begin{pmatrix}0\\ \tau_{xz}\\ \tau_{yz}\\ \tau_{zz}\\ u_x\tau_{xz}+u_x\tau_{yz}+u_x\tau_{zz}-q_z\end{pmatrix},$$

$$\tau_{xx}=\frac{2}{3}\mu\left(2\frac{\partial u_x}{\partial x}-\frac{\partial u_y}{\partial y}-\frac{\partial u_z}{\partial z}\right),$$

$$\tau_{yx}=\tau_{xy}=\mu\left(\frac{\partial u_x}{\partial y}+\frac{\partial u_y}{\partial x}\right),$$

$$\tau_{zx}=\tau_{xz}=\mu\left(\frac{\partial u_x}{\partial z}+\frac{\partial u_z}{\partial x}\right),$$

$$\tau_{yy}=\frac{2}{3}\mu\left(2\frac{\partial u_y}{\partial y}-\frac{\partial u_x}{\partial x}-\frac{\partial u_z}{\partial z}\right),$$

$$\tau_{zz}=\frac{2}{3}\mu\left(2\frac{\partial u_z}{\partial z}-\frac{\partial u_y}{\partial y}-\frac{\partial u_x}{\partial x}\right),$$

$$\tau_{yz}=\tau_{zy}=\mu\left(\frac{\partial u_z}{\partial y}+\frac{\partial u_y}{\partial z}\right),$$

$$q_x=-k\frac{\partial T}{\partial x},$$

$$q_y=-k\frac{\partial T}{\partial y},$$

$$q_z=-k\frac{\partial T}{\partial z}. \quad \text{(A.2)}$$

(2) In the cylindrical coordinates, Equation (A.1) is rewritten as follows:

$$\frac{\partial U}{\partial t}+\frac{\partial (E-V_x)}{\partial x}+\frac{\partial (F-V_\theta)}{r\partial \theta}+\frac{\partial r(G-V_r)}{r\partial r}=S. \quad \text{(A.3)}$$

In Equation (A.3),

$$U = \begin{pmatrix} \rho \\ \rho u_x \\ \rho u_\theta \\ \rho u_r \\ \rho E \end{pmatrix},$$

$$E = \begin{pmatrix} \rho u_x \\ \rho u_x u_x + p \\ \rho u_\theta u_x \\ \rho u_r u_x \\ \rho H u_x \end{pmatrix},$$

$$F = \begin{pmatrix} \rho u_\theta \\ \rho u_x u_\theta \\ \rho u_\theta u_\theta + p \\ \rho u_r u_\theta \\ \rho H u_\theta \end{pmatrix},$$

$$G = \begin{pmatrix} \rho u_r \\ \rho u_x u_r \\ \rho u_\theta u_r \\ \rho u_r u_r + p \\ \rho H u_r \end{pmatrix},$$

$$V_x = \begin{pmatrix} 0 \\ \tau_{xx} \\ \tau_{\theta x} \\ \tau_{rx} \\ u_x \tau_{xx} + u_\theta \tau_{\theta y} + u_r \tau_{rx} - q_x \end{pmatrix},$$

$$V_\theta = \begin{pmatrix} 0 \\ \tau_{x\theta} \\ \tau_{\theta\theta} \\ \tau_{r\theta} \\ u_x \tau_{x\theta} + u_\theta \tau_{\theta\theta} + u_r \tau_{r\theta} - q_\theta \end{pmatrix},$$

$$V_r = \begin{pmatrix} 0 \\ \tau_{\theta r} \\ \tau_{yr} \\ \tau_{rr} \\ u_x \tau_{xr} + u_\theta \tau_{\theta r} + u_r \tau_{rr} - q_r \end{pmatrix},$$

$$\tau_{xx} = \frac{2}{3}\mu\left(2\frac{\partial u_x}{\partial x} - \frac{\partial r u_r}{r\partial r} - \frac{\partial u_\theta}{r\partial\theta}\right),$$

$$\tau_{x\theta} = \mu\left(\frac{\partial u_\theta}{\partial x} + \frac{\partial u_x}{r\partial\theta}\right),$$

$$\tau_{rx} = \tau_{xr} = \mu\left(\frac{\partial u_r}{\partial x} + \frac{\partial u_x}{\partial r}\right),$$

$$\tau_{\theta\theta} = \frac{2}{3}\mu\left(2\frac{\partial u_\theta}{r\partial\theta} - \frac{\partial r u_r}{r\partial r} - \frac{\partial u_x}{\partial x}\right) + \mu\frac{2u_r}{r},$$

$$\tau_{rr} = \frac{2}{3}\mu\left(2\frac{\partial r u_r}{r\partial r} - \frac{\partial u_\theta}{r\partial\theta} - \frac{\partial u_x}{\partial x}\right) - \frac{2\mu u_r}{r},$$

$$\tau_{r\theta} = \tau_{\theta r} = \mu\left(\frac{\partial r u_\theta}{r\partial r} + \frac{\partial u_r}{r\partial\theta}\right) - \frac{2\mu u_\theta}{r},$$

$$S = \begin{pmatrix} 0 \\ 0 \\ \dfrac{-\rho u_\theta u_r + \tau_{\theta r}}{r} \\ \dfrac{\rho u_\theta u_\theta + p - \tau_{\theta\theta}}{r} \\ 0 \end{pmatrix}. \tag{A.4}$$

(3) Ignoring the tangential velocity u_θ and vertical velocity u_x, Equation (A.3) is rewritten to the N-S equation of radial flow and expanded as follows:

$$\begin{aligned} &\frac{\partial \rho}{\partial t} + \frac{\partial r\rho v_r}{r\partial r} = 0, \\ &\frac{\partial \rho v_r}{\partial t} + \frac{\partial r(\rho v_r v_r + p - \tau_{rr})}{r\partial r} = \frac{p}{r}, \\ &\frac{\partial \rho E}{\partial t} + \frac{\partial r(\rho H v_r - v_r \tau_{rr} + q_r)}{r\partial r} = \rho q. \end{aligned} \tag{A.5}$$

In the equation, u_x represents velocity in the x direction, u_y represents velocity in the y direction, u_z represents velocity in the z direction, u_θ represents velocity in $_\theta$ angular tangential, u_r represents radial velocity in the r direction, q_x represents volume flow in the x direction, u_y represents volume flow in the y direction, and u_z represents volume flow in the z direction.

Data Availability

The experimental data used to support the findings of this study are included within the manuscript.

Conflicts of Interest

The authors declared that there is no conflict of interest.

Acknowledgments

This research was funded by the Key Research and Development Program of Ningxia, grant number: 2021BEG03020.

References

[1] J. Li, B. Guo, D. Gao, and C. Ai, "The effect of fracture-face matrix damage on productivity of fractures with infinite and finite conductivities in shale-gas reservoirs," *SPE Drilling & Completion*, vol. 27, no. 3, pp. 347–353, 2012.

[2] D. J. Romero, P. P. Valkó, and M. J. Economides, "Optimization of the productivity index and the fracture geometry of a stimulated well with fracture face and choke skins," *SPE Production & Facilities*, vol. 18, no. 1, pp. 57–64, 2003.

[3] L. Pingya, M. Yingfeng, and S. Shihong, "Some problems in the exploration and exploitation low permeability of oil and gas resources in China," in *SPE International Oil and Gas Conference and Exhibition in China*, Beijing, China, 1998.

[4] R. R. Angel, "Volume requirements for air or gas drilling," *Transactions of AIME*, vol. 210, no. 1, pp. 325–330, 1957.

[5] R. A. Cunningham and J. G. Eenink, "Laboratory study of effect of overburden, formation, and mud column pressure on drilling rate of permeable formations," *Transactions of the AIME*, vol. 217, no. 1, pp. 9–17, 1959.

[6] W. C. Lyons, B. Guo, R. L. Graham, and G. D. Hawley, *Air and Gas Drilling Manual*, Elsevier Publishing Company, third edition, 2009.

[7] B. Guo, G. Li, J. Song, and J. Li, "A feasibility study of gas-lift drilling in unconventional tight oil and gas reservoirs," *Journal of Natural Gas Science and Engineering*, vol. 37, pp. 551–559, 2017.

[8] B. Guo, J. Shan, and Y. Feng, "Productivity of blast-fractured wells in liquid-rich shale gas formations," *Journal of Natural Gas Science and Engineering*, vol. 18, pp. 360–367, 2014.

[9] J. Li, B. Guo, and B. Li, "A closed form mathematical model for predicting gas temperature in gas- drilling unconventional tight reservoirs," *Journal of Natural Gas Science and Engineering*, vol. 27, pp. 284–289, 2015.

[10] Z. Yong and Z. Jianliang, "Technical improvements and application of air-lift reverse circulation drilling technology to ultra-deep geothermal well," *Procedia Engineering*, vol. 73, pp. 243–251, 2014.

[11] J. E. Warren and P. J. Root, "The behavior of naturally fractured reservoirs," *SPE Journal*, vol. 3, no. 3, pp. 245–255, 1963.

[12] R. Abdelazim and S. S. Rahman, "Estimation of permeability of naturally fractured reservoirs by pressure transient analysis: an innovative reservoir characterization and flow simulation," *Journal of Petroleum Science and Engineering*, vol. 145, pp. 404–422, 2016.

[13] S. J. D. Sofla, B. Pouladi, M. Sharifi, B. Shabankareian, and M. K. Moraveji, "Experimental and simulation study of gas diffusion effect during gas injection into naturally fractured reservoirs," *Journal of Natural Gas Science and Engineering*, vol. 33, pp. 438–447, 2016.

[14] H. Kazemi, "Pressure transient analysis of naturally fractured reservoirs with uniform fracture distribution," *SPE Journal*, vol. 9, no. 4, pp. 451–462, 1969.

[15] K. Slimani and D. Tiab, "Pressure transient analysis of partially penetrating wells in a naturally fractured reservoir," *Journal of Canadian Petroleum Technology*, vol. 47, no. 5, pp. 63–69, 2008.

[16] W. Yonghui, L. Cheng, S. Huang et al., "A semi-analytical model for simulating fluid flow in naturally fractured reservoirs with non-homogeneous vugs and fractures," *SPE Journal*, vol. 24, no. 1, pp. 334–348, 2019.

[17] D. Xin, Q. Li, L. Zhiwei et al., "Pressure transient analysis for multi-vug composite fractured vuggy carbonate reservoirs," *Journal of Petroleum Science and Engineering*, vol. 193, article 107389, 2020.

[18] R.-S. Nie, X. Fan, M. Li et al., "Modeling transient flow behavior with the high velocity non-Darcy effect in composite naturally fractured-homogeneous gas reservoirs," *Journal of Natural Gas Science and Engineering*, vol. 96, article 104269, 2021.

[19] J. Adachi, E. A. Siebrits, J. D. Peirce, and J. Desroches, "Computer simulation of hydraulic fractures," *International Journal of Rock Mechanics and Mining Sciences*, vol. 44, no. 5, pp. 739–757, 2007.

[20] S. Mahmoodi, M. Abbasi, and M. Sharifi, "New fluid flow model for hydraulic fractured wells with non-uniform fracture geometry and permeability," *Journal of Natural Gas Science and Engineering*, vol. 68, article 102914, 2019.

[21] L. Jiang, J. Liu, T. Liu, and D. Yang, "Semi-analytical modeling of transient pressure behaviour for a fractured vertical well with hydraulic/natural fracture networks by considering stress- sensitive effect," *Journal of Natural Gas Science and Engineering*, vol. 82, article 103477, 2020.

[22] X. Youjie, X. Li, Q. Liu, and X. Tan, "Pressure performance of multi-stage fractured horizontal well considering stress sensitivity and dual permeability in fractured gas reservoirs," *Journal of Petroleum Science and Engineering*, vol. 201, article 108154, 2021.

[23] G. Daihong, D. Ding, Z. Gao, L. Leng Tian, and C. X. Liu, "A fractally fractional diffusion model of composite dual-porosity for multiple fractured horizontal wells with stimulated reservoir volume in tight gas reservoirs," *Journal of Petroleum Science and Engineering*, vol. 173, pp. 53–68, 2019.

[24] H. Liu, X. Zhao, X. Tang, B. Peng, J. Zou, and X. Zhang, "A discrete fracture-matrix model for pressure transient analysis in multistage fractured horizontal wells with discretely distributed natural fractures," *Journal of Petroleum Science and Engineering*, vol. 192, article 107275, 2020.

[25] X. H. Wang, L. Li, M. Wang, Z. F. Liu, and A. F. Shi, "A discrete fracture model for two-phase flow involving the capillary pressure discontinuities in fractured porous media," *Advances in Water Resources*, vol. 142, article 103607, 2020.

[26] Y. Zhao, L. Guang, L. Zhang, Y. Wei, J. Guo, and C. Chang, "Numerical simulation of shale gas reservoirs considering discrete fracture network using a coupled multiple transport mechanisms and geomechanics model," *Journal of Petroleum Science and Engineering*, vol. 195, article 107588, 2020.

[27] D. Xin, Q. Li, Y. Xian, and L. Detang, "Fully implicit and fully coupled numerical scheme for discrete fracture modeling of shale gas flow in deformable rock," *Journal of Petroleum Science and Engineering*, vol. 205, article 108848, 2021.

[28] L. D. Connell, L. Meng, and Z. Pan, "An analytical coal permeability model for tri-axial strain and stress conditions," *International Journal of Coal Geology*, vol. 84, no. 2, pp. 103–114, 2010.

[29] D. Li, J. Y. Wang, W. Zha, and D. Lu, "Pressure transient behaviors of hydraulically fractured horizontal shale-gas wells

by using dual-porosity and dual-permeability model," *Journal of Petroleum Science and Engineering*, vol. 164, pp. 531–545, 2018.

[30] Y.-l. Zhao, L.-h. Zhang, J.-z. Zhao, J.-x. Luo, and B.-n. Zhang, ""Triple porosity" modeling of transient well test and rate decline analysis for multi-fractured horizontal well in shale gas reservoirs," *Journal of Petroleum Science and Engineering*, vol. 110, pp. 253–262, 2013.

[31] J. Rashidinia, M. Ghasemi, and Z. Mahmoodi, "Spline approach to the solution of a singularly-perturbed boundary-value problems," *Applied Mathematies and Computation*, vol. 189, no. 1, pp. 72–78, 2007.

[32] S. C. Rao and M. Kumar, "Exponential B-spline collocation method for self-adjoint singularly perturbed boundary value problems," *Applied Numerical Mathematies*, vol. 58, no. 10, pp. 1572–1581, 2008.

[33] S. Momani, "An algorithm for solving the fractional convection-diffusion equation with nonlinear source term," *Communications in Nonlinear Science and Numerical Simulation*, vol. 12, no. 7, pp. 1283–1290, 2007.

[34] S. G. Chefranov and A. S. Chefranov, "The new exact solution of the compressible 3D Navier-Stokes equations," *Communications in Nonlinear Science and Numerical Simulation*, vol. 83, article 105118, 2020.

[35] Y. Cho and H. Kim, "On classical solutions of the compressible Navier-Stokes equations with nonnegative initial densities," *manuscripta mathematica*, vol. 120, no. 1, pp. 91–129, 2006.

[36] E. Feireisl, *Dynamics of Viscous Compressible Fluids*, Oxford University Press, Oxford, 2003.

[37] A. Luchko and R. Gorenflo, *The Initial Value Problem for Some Fractional Differential Equations with the Caputo Derivative, Preprint Series A08–98*, Freic Universitat Berlin: Fachbreich Mathematik und Informatik, 1998.

[38] M. Caputo, "Linear models of dissipation whose Q is almost frequency independent–II," *Geophysical Journal International*, vol. 13, no. 5, pp. 529–539, 1967.